Hindawi
Concepts in Magnetic Resonance Part B, Magnetic Resonance Engineering
Volume 2022, Article ID 7332324, 10 pages
https://doi.org/10.1155/2022/7332324

Research Article

Development of Electron Paramagnetic Resonance Magnet System for *In Vivo* Tooth Dosimetry

Kwon Choi,[1] **ChangUk Koo**,[1] **JeongHun Oh**,[1] **Jong In Park**,[2] **Hiroshi Hirata**,[3] **and Sung-Joon Ye**[4,5,6,7]

[1]*Program in Biomedical Radiation Sciences, Graduate School of Convergence Science and Technology, Seoul National University, Seoul 08826, Republic of Korea*
[2]*Korea Research Institute of Standards and Science, Daejeon 34113, Republic of Korea*
[3]*Division of Bioengineering and Bioinformatics, Faculty of Information Science and Technology, Hokkaido University, North 14, West 9, Kita-Ku, Sapporo 060-0814, Japan*
[4]*Department of Applied Bioengineering, Graduate School of Convergence Science and Technology, Seoul National University, Seoul 08826, Republic of Korea*
[5]*Research Institute of Convergence Science, Seoul National University, Seoul 08826, Republic of Korea*
[6]*Advanced Institute of Convergence Technology, Seoul National University, Suwon 16229, Republic of Korea*
[7]*Biomedical Research Institute, Seoul National University Hospital, Seoul 03080, Republic of Korea*

Correspondence should be addressed to Sung-Joon Ye; sye@snu.ac.kr

Received 11 March 2022; Accepted 6 May 2022; Published 27 May 2022

Academic Editor: Xiaodong Yang

As part of a homebuilt continuous wave electron paramagnetic resonance (EPR) spectrometer operating at 1.2 GHz, a magnet system for *in vivo* tooth dosimetry was developed. The magnet was designed by adopting NdFeB permanent magnet (PM) for the main magnetic field generation. For each pole of the magnet, 32 cylindrical PMs were arranged in 2 axially aligned ring arrays. The pole gap was 18 cm, which was wide enough for a human head breadth. The measured magnetic field was compared with the magnetic field distribution calculated in a finite element method (FEM) simulation. EPR spectra of intact human teeth irradiated 5 and 30 Gy were measured for the performance test with the developed magnet system and spectrometer. The measured mean magnetic flux density was estimated to be 44.45 mT with homogeneity of 1,600 ppm in a 2 cm diameter of the spherical volume of the XY plane, which was comparable to the FEM simulation results. The sweep coefficient of the magnetic field sweep coil was 0.35 mT per Ampere in both the measurement and FEM simulation. With ±9 A current, the sweep range was 5.7 mT, which was sufficiently wide to measure the tooth radiation-induced signal (RIS) and reference material. The peak-to-peak amplitude of the measured modulation field was 0.38 mT at the center of the magnet. With the developed magnet fully integrated into an EPR system, the EPR spectra of 5 and 30 Gy irradiated teeth were successfully acquired. The developed magnet system showed sufficiently acceptable performance in terms of magnetic flux density and homogeneity. The EPR spectrum of tooth RIS could be measured *ex vivo*. The RIS of 5 and 30 Gy irradiated teeth was clearly distinguishable from intact human teeth.

1. Introduction

The triage of a large population is a critical social demand when a nuclear accident occurs, such as Chernobyl disaster in 1986 and Fukushima Daiichi nuclear accident in 2011. While the number of potential patients is large, the individual radiation damage is widely distributed from a slight to a life-threatening dose. Depending on the degree of significance, proper management and treatment of injuries are urgently required [1]. This is why triage is critically demanded to assess the radiation dose. In addition, a quick assessment of radiation dose for individuals is required to be performed on-site, but technologies for such are limited. The current gold standard for dose assessment in exposed individuals is a dicentric scoring analysis [2]. However, dicentric analysis is a laborious and time-consuming method that requires 72–96 h for lymphocyte culture and manual scoring by an expert. Even with advanced improvements, such as automated dicentric analysis, it takes 48 h only for cell culturing [3].

In vivo electron paramagnetic resonance (EPR) tooth dosimetry is a currently available technique for radiation dose assessment for human subjects noninvasively. EPR has been employed in radiation dosimetry by quantifying the amount of radicals generated by ionizing radiation [4]. Ionizing radiation generates stable CO_2^- radicals in calcified human tissues, such as tooth enamel and bone. *In vivo* EPR tooth dosimetry is useful, especially in radiological accidents, where most potential victims do not possess appropriate dosimeters for its expeditiousness [5]. It can rapidly assess an exposure dose in 10 min, including 5 min of measurement and 5 min of assessment. Such advantages have been exploited to estimate victims' exposure retrospectively in radiation accidents [6–8].

In vivo EPR tooth dosimetry has been extensively studied [5, 9–11]. The *in vivo* method investigates intact human teeth noninvasively without preprocessing to use noninvasiveness, on-site response, and expeditiousness during dose estimation. In the conventional method, a microwave frequency of 9 GHz or higher is used, which is easily absorbed into aqueous material in *in vivo* studies. Thus, most *in vivo* studies chose low frequencies around 1 GHz to avoid the interference of water [5, 9]. Some scholars tried using X-band frequency for *in vivo* tooth dosimetry together with a modified X-band resonator [10, 11]. Owing to the lack of commercially available spectrometers for human studies, specific devices have to be developed for *in vivo* studies aiming at human applications. Hirata et al. [12] developed an electronically tunable resonator for *in vivo* EPR measurement. Guo et al. [10, 11] also developed a resonator to measure only *in vivo* tooth dosimetry using X-band.

In addition, the *in vivo* method is relatively easy for unskilled workers to assess the radiation dose of an exposed person, making *in vivo* EPR tooth dosimetry suitable for an on-site patient triage tool. To deploy EPR-based dosimetry instruments to places close to a disaster area or the shelter of evacuees, EPR instruments should be mobile and easily operated. However, the magnet of an EPR spectrometer and its power supply are generally heavy. This is an obstacle to transfer the EPR spectrometer from a laboratory to a field near a disaster area.

It is known that using permanent magnet (PM) arrays reduces the weight of the magnet at a low cost [13]. A car-mounted magnetic resonance imaging system for on-site diagnosis has been proposed [14]. The magnet was 200 kg in weight, which was deployable using a car. Swartz et al. [15] developed a deployable EPR spectrometer for *in vivo* tooth dosimetry, including the magnet. The magnet weighed 30 kg [16]. Numerous studies on *in vivo* EPR dosimetry were recently reviewed. Sato-Akaba et al. [17] used small neodymium magnet arrays to form a homogeneous magnetic field for biological EPR imaging. The magnet combined with coils weighed 6 kg. Sirota et al. developed a magnet for pulsed EPR tooth dosimetry by adopting the methodology of *ex situ* nuclear magnetic resonance (NMR) [18]. They also tried *in vivo* tooth dosimetry with another type of magnet under an 11.2 GHz frequency [19].

In this study, we develop a magnet system using PMs with deployable weight for *in vivo* EPR tooth dosimetry. The magnet system for *in vivo* EPR dosimetry is a key component to be developed by in-house users. Although there have been many studies to develop a magnet system for general purposes, including NMR and magnetic hyperthermia, the number of EPR studies describing the development of magnet systems for *in vivo* tooth dosimetry is limited [20–22].

The development described in this study is part of the entire development of an *in vivo* EPR spectrometer for tooth dosimetry. In this study, a magnet system focusing on *in vivo* EPR tooth dosimetry was developed using PMs and copper coils. First, the design and fabrication of the magnet system are described. Then, the performance of the magnet system is evaluated in terms of magnetic flux density and uniformity. Finally, *ex vivo* EPR spectra were measured to verify the magnet system's performance.

2. Materials and Methods

2.1. Design Concept and Required Specifications. As mentioned above, we fabricated an EPR magnet with deployable weight for *in vivo* tooth dosimetry in this study. Therefore, the required specifications are determined from the viewpoint of weight (deployability), pole gap width, main magnetic flux density, magnetic field homogeneity, sweep field width, and amplitude of the modulation field.

For the magnet to be deployable, at least by a car, it should be light enough to be loaded onto a vehicle by one person. Based on the study by Williams et al. [16], the weight should be equal to or lower than 30 kg. The pole gap of the magnet was determined considering the subject's head size. Since the subject's head is located between the pole gap to measure the tooth *in vivo*, a sufficiently wide space should be taken between the two poles of the magnet. This would be 18 cm due to a statistical reason given later in the part where the EPR magnet's design was described.

Meanwhile, the main magnetic flux density, B_0, and homogeneity required for tooth dosimetry should be secured. The B_0 is determined following the microwave frequency used for operation. A high frequency tends to be absorbed by tissues around the measured tooth. As such, frequencies of approximately 1.2 GHz have been adopted as the detection frequencies in several preclinical and clinical systems, compromising sensitivity and detection depth [9]. The required B_0 was calculated to be 42.9 mT. The B_0 field needs to be sufficiently homogeneous over the sample volume [23]. The least required homogeneity of B_0 is determined by the variation of B_0 over the sample volume and the linewidth of the investigated sample. As a rule of thumb, the variation in the magnetic field strength over the sample should be less than 10% of the linewidth of the sample signal [23]. For tooth dosimetry, the linewidth of the radiation-induced signal (RIS) of a tooth is known to be 0.26 mT [9, 24, 25], so the required B_0 variation is 0.026 mT. The scannable range of the magnetic field should include the spectrum of the reference material, 4-oxo-2,2,6,6-tetramethylpiperidine-d_{16}–1-^{15}N-1-oxyl (^{15}N-perdeuterated tempone (^{15}N-PDT), CDN Isotopes, Quebec, Canada) and that of the tooth. The least sweep range required for this is approximately 3.5 mT. The amplitude of RIS of the tooth EPR spectrum is known to be maximized at 0.4 mT field modulation. In our design, a modulation field of 0.4 mT is planned to be applied to the tooth sample location. The modulation frequency should be more than 20 kHz, which is a limitation of audible frequency due to its *in vivo* application.

2.2. EPR Magnet Configuration. Figure 1 shows a schematic design of the EPR magnet system for *in vivo* tooth dosimetry. The magnet system typically comprises PMs, magnetic field sweep coils, and magnetic field modulation coils. PMs are used to generate the Zeeman magnetic field of the L-band (1.2 GHz in this study). In continuous wave (CW) EPR, the spectrum is acquired by scanning magnetic fields around the main magnetic field (B_0). This spectrum is acquired in the presence of an alternating current (AC) magnetic field formed by the magnetic field modulation coils.

B_0 is generally provided by electromagnets in commercial EPR spectrometers using relatively higher frequencies, such as X- or Q-bands. PMs are also available in applications of L-band or lower frequencies, which are broadly used for *in vivo* measurements. Adopting PMs for B_0 has an advantage over electromagnets by reducing the number of devices for electromagnet operation, such as a power supply and cooling system.

Each magnetic field sweep coil comprises two separate axially aligned identical circular coils operated with direct current (DC). By applying DC to the sweep coil, the main magnetic field varies in strength. Each magnetic field modulation coil also comprises two identical circular coils operated with AC.

2.3. EPR Magnet Design. B_0 is static and equivalent to the Zeeman magnetic field of the subject material under investigation. Sintered $Nd_2Fe_{14}B$ (NdFeB) was adopted for the PM material. NdFeB is one of the strongest commercially available PM materials. Cylindrical PMs with a 2.5 cm diameter and 6.2 cm length were used. A total of 32 NdFeB cylindrical magnets were used to make 2 ring arrays, which were axially aligned (blue in Figure 1). Thus, 16 PMs were aligned parallel in each ring. The magnetic flux density generated by the two PM ring arrays is measured at the center region of the two axially aligned rings, where a subject for EPR measurement is positioned.

Between the two axially aligned ring arrays, the space where a subject's head is located for *in vivo* tooth dosimetry should be considered. A homogeneous magnetic field region is formed around the center between the two ring arrays. For *in vivo* measurement, a homogeneous magnetic field should be formed where the upper incisors are located when a subject's head is put between the two poles of the magnet. Some studies statistically estimated the human head size of ethnic groups [26–28]. The head breadth is the maximum horizontal width of the head above the ears and is used to determine the pole gap. From the Civilian American and European Surface Anthropometry Resource (CAESAR) database of North Americans, the maximum head size was estimated to be 17.2 cm in both genders of Caucasian, African, Asian, and Hispanic [28]. The pole gap of 18 cm would be enough to examine most people, although the top 5% of the male group was reported to have a head breadth of 18.2 cm in another study targeting Taiwanese. In this study, the actual gap width between two PM ring arrays was determined to be 19 cm together with a lamination plate of 0.5 cm thickness attached to the inner face of each pole.

The sweep coil has an inner and outer radius of 9.0 and 10.29 cm, respectively, with a width of 3.95 cm, which is placed on the surroundings outside PMs (brown in Figure 1). The EPR measurement for tooth dosimetry requires a sufficient magnetic sweep range to include spectra combined with signals of the reference materials and tooth RIS. In this study, ^{15}N-PDT was used as a reference material, of which the spectrum had two peaks sufficiently included within a 3.5 mT magnetic field sweep when using a 1.2 GHz frequency. To satisfy this requirement with a reasonably tolerable current, 100 turns were wound with a copper wire of 2.2 mm diameter on each side of the sweep coil. The gap between both sides of the coils was the same as that of PMs. The number of turns and diameter of the coils were determined by the guidance of the finite element analysis (FEM) simulation stated below.

The magnetic field modulation coil operates at 21.2 kHz. The modulation coil has an inner and outer radius of 3.3 and 3.97 cm, respectively, with a width of 3.6 cm, which is placed inside the PM ring arrays (red in Figure 1). Eighty-two turns are wound with a copper wire of 1.6 mm diameter on each side. Owing to the characteristic of AC magnetic field inducing eddy current in adjacent conductive materials, the parts nearby were built with nonconductive materials, except for coils and PMs.

2.4. Analytical Calculation of Magnetic Flux Density of PMs. At the design stage, B_0 was calculated to be 42.9 mT assuming $\nu = 1.2$ GHz when g of the radiation-induced radical of the tooth was approximately 2.0. Thus, the grade of the NdFeB magnet was determined to adjust B_0 close to 42.9 mT.

To adjust the central magnetic field to the Zeeman magnetic field, the magnetic field generated by PMs was calculated. The central magnetic field was calculated as the sum of the magnetic fields of each PM. The remanent flux density, B_r, of PM was determined as a nominal value of 1.31 T, which was close to the NdFeB grade of N42. The details of this calculation are described in Appendix.

2.5. Magnetic Field Simulation. COMSOL Multiphysics (version 5.6, COMSOL Inc., Stockholm, Sweden) was employed to guide the design of the magnet system.

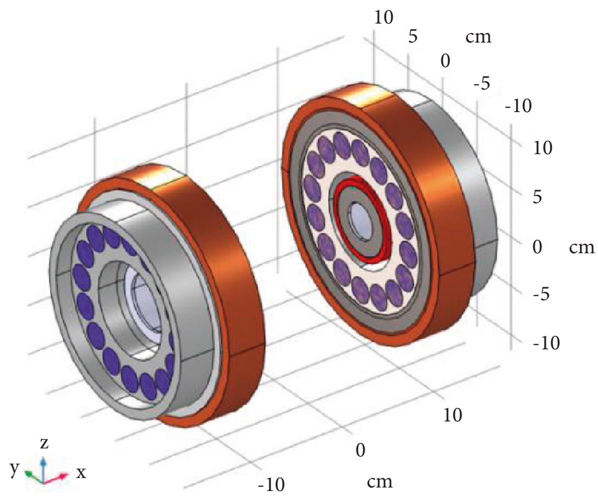

Figure 1: A schematic design of EPR magnet system for *in vivo* tooth dosimetry: the magnet system typically comprises PMs (blue), sweep (brown), and modulation coils (red). It should be noted that the direction of the main magnetic field is on the X-axis.

COMSOL Multiphysics is a commercial FEM software designed to calculate various physical phenomena [29].

For electromagnetic simulation, the physics interface *magnetic field (mf)* available from *AC/DC module* was adopted to compute the magnetic field. The geometry of the magnet system in FEM simulation was simplified to save calculation time. The geometry included PMs, magnetic field modulation coils, modulation coil reels, magnetic field sweep coils, and sweep coil reels. Although the sweep and modulation coil geometries could comprise a torus for each turn of the coil wire, the coils were simplified into tubes. Otherwise, the torus geometry would require significant computational time to calculate a large number of meshes composing tori. The coils were defined using the *multiturn coil* feature. Nonmagnetic components, including the casing and cover, were omitted. Materials applied for each component are listed in Table 1.

2.6. Magnetic Field Measurement. A magnetic flux density of PMs was measured over a 2 cm diameter of a spherical volume (DSV) at the center of the magnet. According to a dental study, the dimension of the human upper incisor in the oral cavity is 8.73–9.3 mm in width and 10.4–11.2 mm in length [30]. Thus, a 2 cm DSV is wide enough to cover the two upper incisors in a subject's oral cavity. For conservative assessment, the DSV was larger than the volume occupied by the two upper incisors by a wide margin. The homogeneity was calculated from the following equation:

$$\text{Homogeneity} = \frac{B_{\text{max}} - B_{\text{min}}}{B_{\text{mean}}} \times 10^6 \text{ [ppm]}. \quad (1)$$

A gaussmeter (DTM-151 Digital Teslameter, Group 3 Technology, Auckland, New Zealand), to which a hall probe (MPT-141 Hall Probe, Group 3 Technology, Auckland, New Zealand) was attached on a platform moving with a conveyer belt, was used to measure the magnetic field. Magnetic flux density from −7 to 7 cm on the X-axis and −5 cm to 5 cm on the Y-axis at the center of the magnet was measured. In addition to the volume data included in 2 cm DSV, the magnetic flux density on X-and Y-line profiles was measured for comparison with the FEM results.

The magnetic flux density of a modulation coil was measured using a search coil magnetometer along the X- and Y-axis around the magnet's geometric center. The search coil comprised ten turn copper coils with a radius of 3.82 mm. The region from −3.5 to 3.5 cm along each axis was measured at a 0.5 cm increment. The magnetometer was connected to an oscilloscope so that the peak-to-peak amplitude of the induced voltage was measured. The strength of the modulation field was evaluated by converting the voltage into the magnetic field.

2.7. EPR Spectrum Acquisition. An EPR spectrum was acquired to verify the performance of the magnet system combined with an EPR system for *in vivo* tooth dosimetry that had been developed at Seoul National University. The magnet pole gap was adjusted to 18.4 cm to lower B_0 closer to the calculated value of 42.9 mT.

The spectrometer system used to acquire EPR spectra is comprised of the developed magnet system, a spectrometer controller system, a microwave bridge, and a tunable resonator (Figure 2(a)). The spectrometer systems except for the developed magnet were tested using a magnet that was described in our previous paper [31]. The magnet system's sweep coils were operated with a bipolar power supply controlled by a controller system. The modulation coils were connected to an amplifier, to which a 21.2 kHz input signal was supplied from the controller system. The acquired data was transmitted to the receiver of the controller.

The circuit connection of the modulation and sweep coils is shown in Figure 2(b). To operate the modulation coils (L_{M1} and L_{M2} in Figure 2(b)) at 21.2 kHz, an LC series

Table 1: Material properties used in COMSOL FEM simulation.

	Relative permeability	Relative permittivity	Electrical conductivity [S/m]	Component
Air	1.0	1.0	0	Ambient space
Copper	1.0	1.0	0	Sweep and modulation coils
MC nylon	1.0	1.0	1.0×10^{-6}	Coil reels, cases
NdFeB	1.05	1.0	5.88×10^{5}	PMs

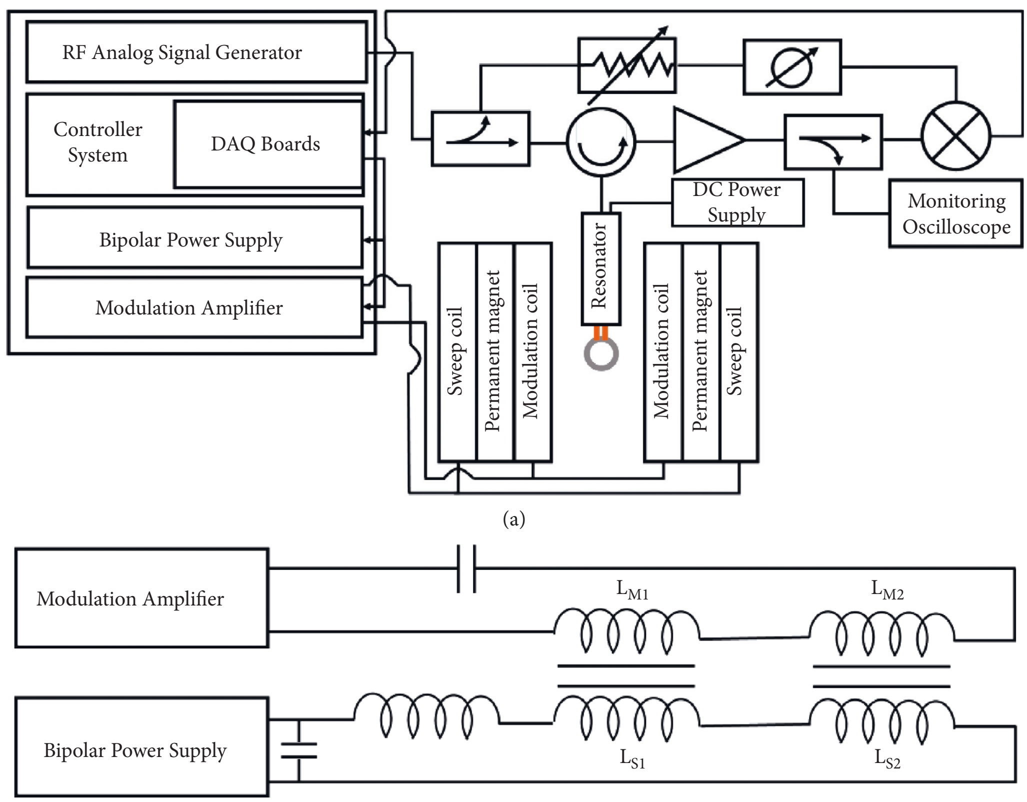

Figure 2: EPR spectrometer connection. (a) A schematic of EPR spectrometer for *in vivo* tooth dosimetry. (b) Circuit connection of modulation coils (L_{M1} and L_{M2}) and sweep coils (L_{S1} and L_{S2}). LC series resonant is used to operate the modulation coils with 21.2 kHz. In sweep coil circuitry, LC low-pass filter is connected to block the AC induced by the AC magnetic field from the modulation coil.

resonance circuit was used. The sweep coils (L_{S1} and L_{S2} in Figure 2(b)) were located close to the modulation coil so that AC was induced on it by the AC magnetic field. This induces not only unintended AC on the sweep coils but also the AC magnetic loss of the modulation field. To reduce this, an LC low-pass filter was connected to the sweep coils.

The EPR spectrum was accumulated ten times for 3 s for each field sweep. Ten spectra were collected for each sample. The peak-to-peak amplitude of the first harmonic signal was estimated. The RIS of two intact human upper incisors was measured after 5 and 30 Gy X-ray irradiation for each. As a reference material, ^{15}N PDT was prepared in a thin Teflon tube after diluting to 0.1 mM.

3. Results and Discussion

3.1. Characteristics of Prototype Magnet System. In this section, the actual characteristics of the described magnet system are described briefly. The total weight of the magnet was 22 kg. The weight is 27% lighter than that of the *in vivo* tooth dosimetry study by Williams et al. [16]. The pole gap width was 18 cm. The main magnetic field was measured to be 44.5 mT at 2 cm DSV of the magnet system's center. Its homogeneity was 0.07 mT in B_0 variation measured along the X-axis in the 2 cm DSV, but it was estimated to be useable, approximately satisfying the 0.026 mT requirement when a tooth is the subject of measurement. The sweep width was 5.7 mT in the current range of ±9 A, sufficiently requiring the aimed specification. The modulation field amplitude was 0.38 mT.

3.2. The Magnet System Building. The designed magnet system was manufactured by Hanmi Techwin, Siheung, Republic of Korea. The developed magnet system is shown in Figure 3. The sweep and modulation coils were independently manufactured and assembled so that they are

(a)

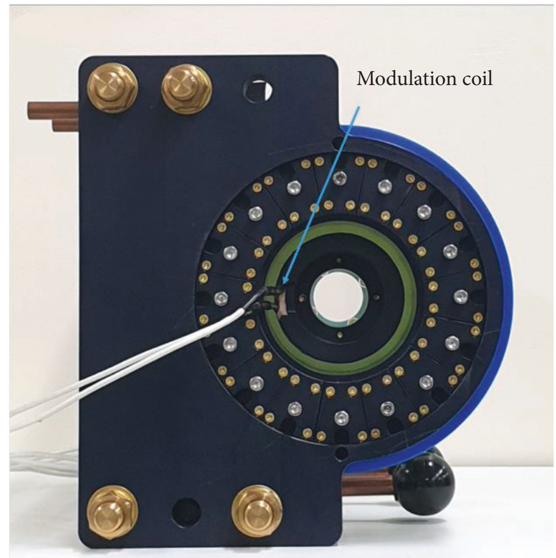

(b)

Figure 3: Manufactured magnet system for *in vivo* EPR tooth dosimetry. PMs are invisible from the outside. (a) Sweep coils are exposed from the front view. (b) Parts of the modulation coils and their wiring are shown from the side view.

independently exchangeable in case of malfunction. The sweep coils are located at the outermost location of the magnet system, whereas the PMs are invisible from the outside (Figure 3(a)). From the side view of the magnet system, some modulation coils and their wiring are seen (Figure 3(b)). The modulation coils are wound with reels made of monomer casting nylon, and their outer sides are exposed to air. All metallic parts, except PMs and coils, were made of brass or stainless steel, which are nonmagnetic. The pole gap has a minimum of 17.8 cm and is extendable up to 19 cm by adjusting 16 hexagon nuts and fixing the location of both sides of the magnet system.

3.3. Prototype Magnet System. The magnetic flux density profiles along the X- and Y-axis are presented in Figure 4 for comparison of the measurement and FEM simulation values. The three profiles in each of Figures 4(a)–4(d) correspond to PMs only and sweep coils operating ±4 A. The mean values and homogeneity of the magnetic field density profiles are summarized in Table 2. As described in Appendix, the analytical calculation was performed to confirm the magnetic flux density of PMs. The measured homogeneities were higher, especially in Figure 4(d), due to the inevitable vibration of a hall sensor during measurements.

After smoothing the profiles with the moving average method, the homogeneity of the Y-axis and XY plane became 337 and 1600 ppm, respectively.

With the smoothed measured data in the Y-axis, the B_0 variation was 0.014 mT, which satisfied the requirement of less than 0.026 mT. However, the raw B_0 variation in the XY plane was 0.07 mT and not satisfactory to the homogeneity requirement. As mentioned earlier, the actual B_0 variation was smaller than this; the homogeneity was calculated conservatively within a volume larger than the tooth. The B_0 variation of the XY plane is 0.028 mT if calculated in the region of 1 cm on the X-axis and of 0.2 cm on the Y-axis around the geometric center. This is nearly satisfactory to the 10% linewidth requirement of RIS. This region could be applied only when one incisor is located at the center.

The magnet system was designed to adjust its pole gap between 18 and 19 cm in case of a situation requiring a change of B_0 strength, which is often caused by a difference (or error) in the remanent flux density of PM from the nominal value. The variation of magnetic flux density versus pole gap distance was calculated in the 2 cm DSV via FEM simulation (Table 3). As the pole gap varied from 18 to 19 cm, B_0 decreased from 43.5 to 41.2 mT. To tune at the 1.2 GHz system frequency of the entire EPR spectrometer, the pole gap was determined to be 18.4 cm.

3.4. Sweep Coil. The magnetic flux density of the sweep coils was measured in the XY plane. The measurement values were compared with FEM simulation values (Figure 4). The mean value and homogeneity with a current in the sweep coil are listed in Table 4. After smoothing the measured Y-axis line profile, the homogeneity became 999 and 611 ppm for −4 and 4 A, respectively. The mean value and homogeneity on the XY plane were evaluated as 45.85 mT and 1381 ppm for 4 A and 43.30 mT and 2350 ppm for −4 A after smoothing the measured values. The sweep efficiency was measured as 0.35 mT per Ampere in the range of ±4 A. When the current range of ±9 A was applied at the bipolar power supply, the sweep field ranged from −2.9 to 2.8 mT around B_0, which was sufficiently wide to acquire EPR spectra of both tooth RIS and the reference signal of ^{15}N-PDT.

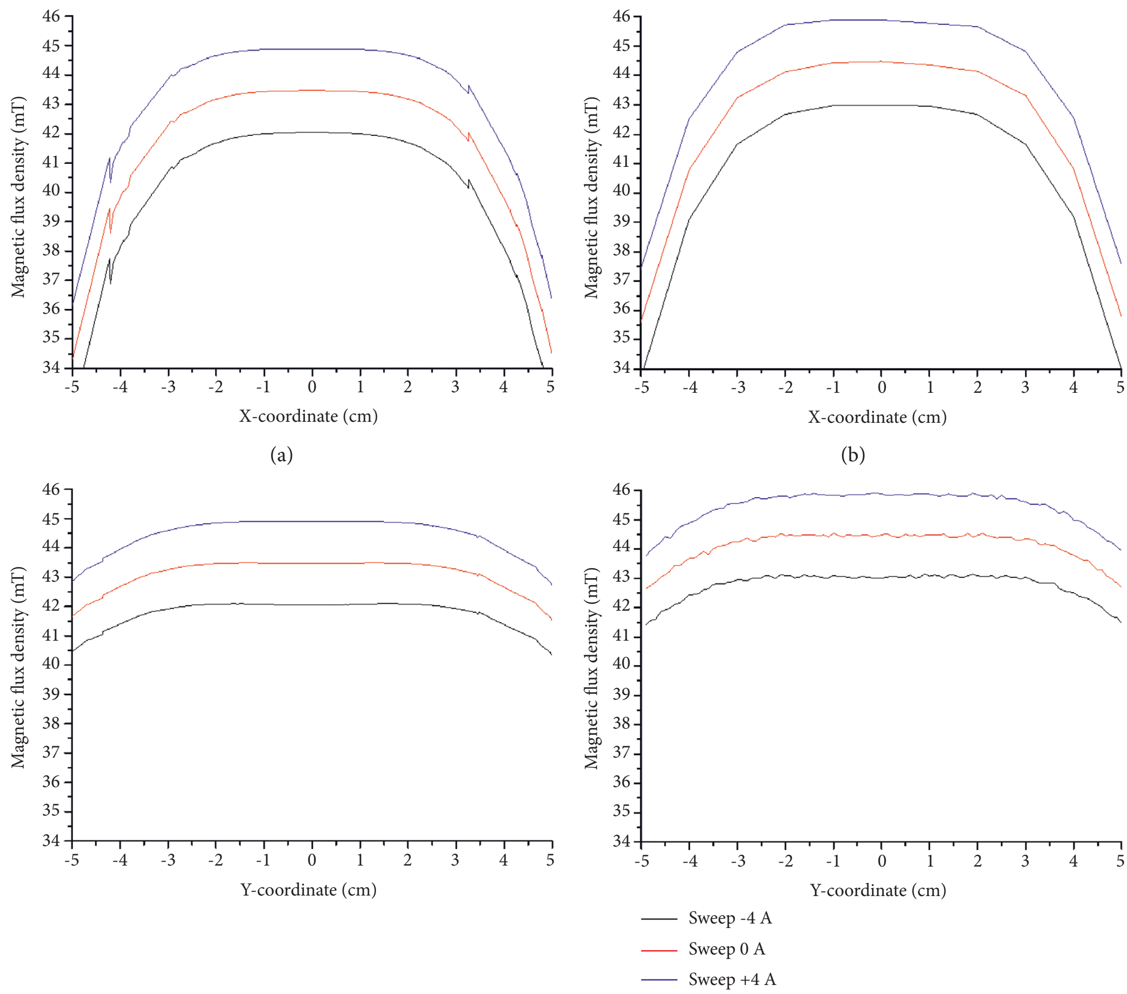

Figure 4: Measured profiles of magnetic flux density along the X- and Y-axis. (a) X-axis profile of FEM results with and without current in sweep coils; (b) X-axis profile of measurement; (c) Y-axis profile of FEM result; (d) Y-axis profile of measurement result. It should be noted that the direction is on the X-axis, and the XY plane is a horizontal midplane between the pole faces.

Table 2: Mean value and homogeneity of magnetic flux density evaluated for 2 cm DSV. The magnetic flux density evaluated from the measurement is significantly nonuniform. After smoothing the measured profiles, the homogeneity of the Y-axis and XY plane is 337 and 1600 ppm, respectively. The X-axis is in the direction where the main magnetic field penetrates the two pole faces. The XY plane is a horizontal midplane between the pole faces.

	X-axis		*Y*-axis		XY plane	
	Mean (mT)	Homogeneity (ppm)	Mean (mT)	Homogeneity (ppm)	Mean (mT)	Homogeneity (ppm)
Measurement	44.43	2701	44.47	2923	44.45	4500
FEM	43.46	829	43.47	374	43.46	1258
Analytical calculation	44.06	891	—	—	—	—

Table 3: Magnetic flux density with pole gap extension. The magnetic field and its homogeneity are estimated for 2 cm DSV.

Pole gap (cm)	Magnetic flux density (mT)	Homogeneity (ppm)
18.0	43.5	2,183
18.2	43.0	2,162
18.4	42.6	2,129
19.0	41.2	2,577

3.5. Modulation Coil Measurements. The measured magnetic flux density profiles of field modulation are shown in Figure 5. The peak-to-peak amplitude was 0.38 mT at the geometric center. In addition, to assess the variation in the magnetic field modulation, the line profiles were measured in the ±1 cm region around the geometric center of the magnet. The homogeneity of the modulation field was 5.7%, 3.6%, and 8.0% along the X-axis, Y-axis, and XY plane, respectively.

TABLE 4: Mean value and homogeneity of magnetic flux density with a current in the sweep coil evaluated for 2 cm DSV. The X-axis is in the direction where the main magnetic field penetrates the two pole faces. The Y-axis is a horizontal plane between two pole faces.

Sweep current	Method	X-axis		Y-axis	
		Mean (mT)	Homogeneity (ppm)	Mean (mT)	Homogeneity (ppm)
−4 A	Measurement	42.98	698	43.05	3,484
	FEM	42.04	1,288	42.06	583
+4 A	Measurement	45.86	2,181	45.86	2,617
	FEM	44.88	400	44.89	268

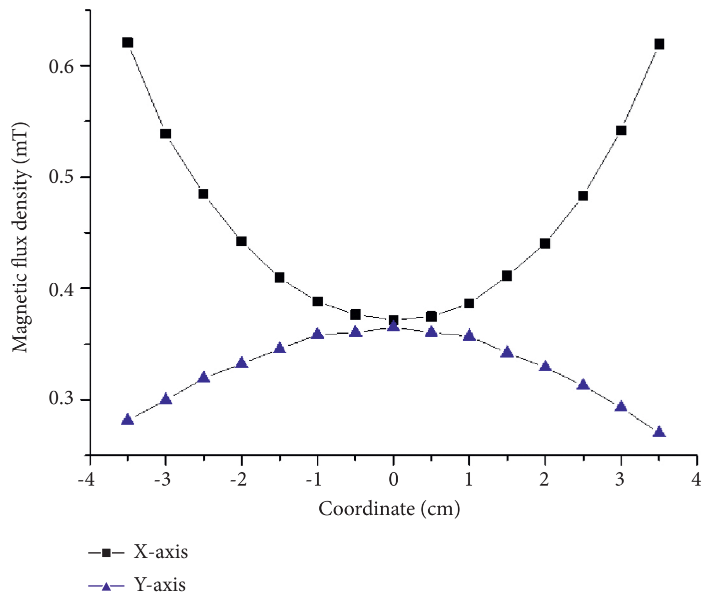

FIGURE 5: Measured line profile of modulation magnetic field peak-to-peak amplitude along the X- and Y-axis. The X-axis is in the direction of the main magnetic field, and the Y-axis is in the horizontal plane between poles.

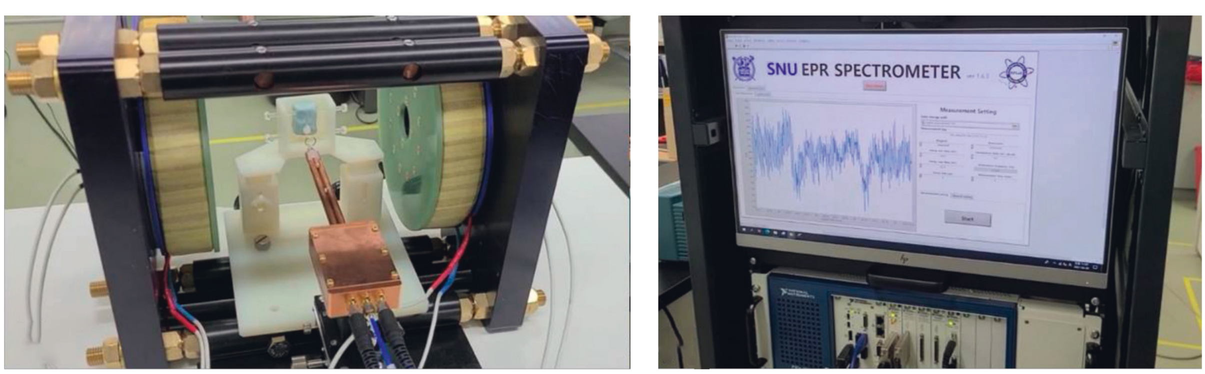

(a) (b)

FIGURE 6: Spectrum acquisition with the developed magnet system: (a) EPR spectra are acquired with a surface coil resonator at the center of the magnet system and (b) the measured signals are collected with the controller system, and the EPR spectrum is acquired.

Compared with data from another group where the homogeneity of the modulation coil was 5%, these values were less uniform [25]. However, when the region was confined to 1 cm on the X-axis and 0.2 cm on the Y-axis where only an incisor can be located, the homogeneity was 1.8%.

3.6. EPR Spectrum Acquisition. To fully test the performance of the magnet system integrated with the entire EPR system, it is essential to acquire the EPR spectrum. A tooth was fixed at the geometric center of the developed magnet system. The surface coil of the resonator was contacted to the surface of the tooth (Figure 6(a)). At each end of the magnetic field sweep, the EPR spectrum measured is shown on the computer's display (Figure 6(b)). Ten sweep data were collected and averaged to produce a spectrum of one tooth.

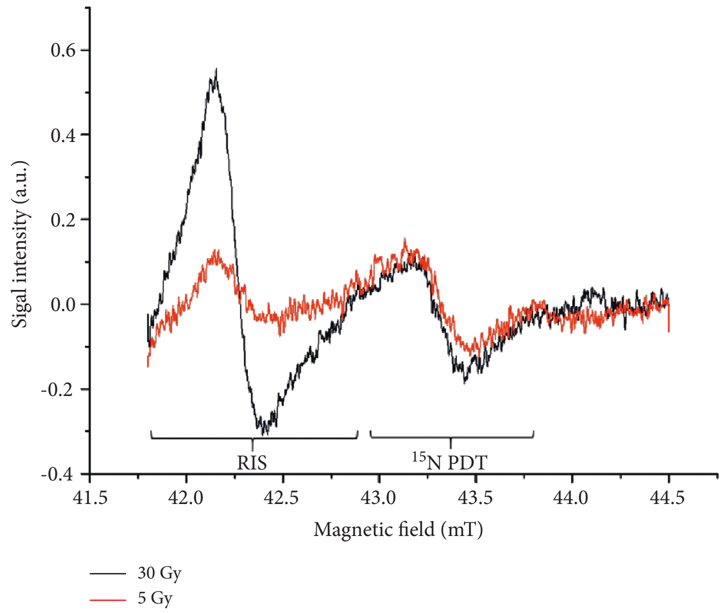

Figure 7: Measured EPR spectrum. Spectrum acquired from 5 (red) and 30 Gy irradiated incisors. Two peaks are shown in each spectrum. RIS of the tooth (left peak) is distinguishable in amplitude. The reference material, ^{15}N PDT (right peak), has the same height in both spectra.

Figure 7 shows EPR spectra acquired from irradiated intact teeth. The spectrum shape was the first derivative of the absorption signal due to magnetic field modulation and phase-sensitive detection. In Figure 7, the left peak was RIS from the tooth, whereas the right one was from the reference material ^{15}N PDT simultaneously measured. Signal amplitudes of the reference signal have the same level in both spectra of 5 and 30 Gy irradiated teeth. RIS spectra of 5 and 30 Gy teeth were distinguishable in amplitude. The peak-to-peak amplitudes of tooth RIS were 0.16 and 0.83 in arbitrary units for 5 and 30 Gy, respectively.

3.7. Thermal Stability of the Magnet. It is known that NdFeB magnets have a temperature coefficient of intrinsic coercivity of approximately −0.10%/°C, which means that the temperature variation of PMs induces the change in the magnetic flux density [32]. The magnetic field shift was observed during long-term EPR measurements. The magnitude of this shift was approximately up to 1.2 mT for the first two hours of operation and then saturated. It seemed due to the temperature rising on PMs mainly by the modulation coils. This magnetic field shift by the heat should be considered when EPR measurements are performed. To prevent the magnetic field shift during the operation, preheating was required when the developed magnet was used. After 2 hours of preheating, the magnetic field shift becomes negligible during further measurements.

4. Conclusions

A magnet system for *in vivo* EPR tooth dosimetry was designed and fabricated in this study. The fabricated magnet system satisfied the specifications required to perform *in vivo* tooth dosimetry. NdFeB PMs were used to generate the main magnetic field, B_0, which was estimated to be 44.5 mT at the geometric center of the magnet. The field homogeneity was sufficient to be used for EPR tooth dosimetry compared to a known RIS linewidth of tooth spectrum. Furthermore, compared with a 0.26 mT linewidth of tooth RIS, the modulation field was sufficiently strong to measure tooth RIS spectra. The range of the sweep coil was 5.7 mT with ±9 A current. It was wide enough to acquire the full EPR spectra of both RIS and ^{15}N-PDT. The EPR spectra of the irradiated teeth were successfully acquired using the fabricated magnet system. The RIS of 5 and 30 Gy irradiated teeth was clearly distinguishable.

Data Availability

The COMSOL simulation data used to support the findings of this study are included within the article.

Conflicts of Interest

The authors declare that they have no conflicts of interest.

Acknowledgments

This work was supported by the Nuclear Safety Research Program through the Korea Foundation of Nuclear Safety (KoFONS) using the financial resources granted by the Nuclear Safety and Security Commission (NSSC) of the Republic of Korea (No. 2003021).

Supplementary Materials

The analytical calculation was performed to confirm the magnetic flux density of PMs at the design stage. (*Supplementary Materials*)

References

[1] S. Akita, "Treatment of radiation injury," *Advances in Wound Care*, vol. 3, pp. 1–11, 2014.

[2] M. E. Berger, D. M. Christensen, P. C. Lowry, O. W. Jones, and A. L. Wiley, "Medical management of radiation injuries: current approaches," *Occupational Medicine*, vol. 56, no. 3, pp. 162–172, 2006.

[3] T. L. Ryan, M. B. Escalona, T. L. Smith, J. Albanese, C. J. Iddins, and A. S. Balajee, "Optimization and validation of automated dicentric chromosome analysis for radiological/nuclear triage applications," *Mutation Research: Genetic Toxicology and Environmental Mutagenesis*, vol. 847, Article ID 503087, 2019.

[4] A. Lund and M. Shiotani, *Applications of EPR in Radiation Research*, Springer, Berlin, Germany, 2014.

[5] B. B. Williams, A. B. Flood, I. Salikhov et al., "In vivo EPR tooth dosimetry for triage after a radiation event involving large populations," *Radiation and Environmental Biophysics*, vol. 53, no. 2, pp. 335–346, 2014.

[6] A. I. Ivannikov, E. Gaillard-Lecanu, F. Trompier et al., "Dose reconstruction by EPR spectroscopy of tooth enamel: application to the population of Zaborie village exposed to high radioactive contamination after the chernobyl accident," *Health Physics*, vol. 86, no. 2, pp. 121–134, 2004.

[7] A. Romanyukha, D. Regulla, E. Vasilenko, and A. Wieser, "South Ural nuclear workers: comparison of individual doses from retrospective EPR dosimetry and operational personal monitoring," *Applied Radiation and Isotopes*, vol. 45, no. 12, pp. 1195–1199, 1994.

[8] N. Nakamura, C. Miyazawa, S. Sawada, M. Akiyama, and A. Awa, "A close correlation between electron spin resonance (ESR) dosimetry from tooth enamel and cytogenetic dosimetry from lymphocytes of Hiroshima atomic-bomb survivors," *International Journal of Radiation Biology*, vol. 73, no. 6, pp. 619–627, 1998.

[9] W. Schreiber, S. V. Petryakov, M. M. Kmiec et al., "In vivo CW-EPR spectrometer systems for dosimetry and oximetry in preclinical and clinical applications," *Applied Magnetic Resonance*, vol. 53, pp. 123–143, 2021.

[10] J. Guo, X. Luan, Y. Tian et al., "The design of X-band EPR cavity with narrow detection aperture for in vivo fingernail dosimetry after accidental exposure to ionizing radiation," *Scientific Reports*, vol. 11, pp. 2883–2888, 2021.

[11] J. Zou, J. Guo, L. Ma et al., "A normalization method of the volume and geometry of tooth for X-band in vivo EPR dosimetry," *Applied Radiation and Isotopes*, vol. 149, pp. 123–129, 2019.

[12] H. Hirata, T. Walczak, and H. M. Swartz, "Electronically tunable surface-coil-type resonator for L-band EPR spectroscopy," *Journal of Magnetic Resonance*, vol. 142, no. 1, pp. 159–167, 2000.

[13] C. Z. Cooley, M. W. Haskell, S. F. Cauley et al., "Design of sparse halbach magnet arrays for portable MRI using a genetic algorithm," *IEEE Transactions on Magnetics*, vol. 54, pp. 1–12, 2018.

[14] M. Nakagomi, M. Kajiwara, J. Matsuzaki et al., "Development of a small car-mounted magnetic resonance imaging system for human elbows using a 0.2 T permanent magnet," *Journal of Magnetic Resonance*, vol. 304, pp. 1–6, 2019.

[15] H. M. Swartz, B. B. Williams, B. I. Zaki et al., "Clinical EPR: unique opportunities and some challenges," *Academic Radiology*, vol. 21, no. 2, pp. 197–206, 2014.

[16] B. B. Williams, R. Dong, A. B. Flood et al., "A deployable in vivo EPR tooth dosimeter for triage after a radiation event involving large populations," *Radiation Measurements*, vol. 46, no. 9, pp. 772–777, 2011.

[17] H. Sato-Akaba, Y. Okada, K. Tsuji, M. C. Emoto, and H. G. Fujii, "Design and fabrication of compact arrayed magnet for biological EPR imaging," *Applied Magnetic Resonance*, vol. 52, no. 8, pp. 1017–1029, 2021.

[18] K. Sirota, Y. Twig, and A. Blank, "Pulsed electron spin resonance ex situ probe for tooth biodosimetry," *Applied Magnetic Resonance*, vol. 44, no. 6, pp. 671–689, 2013.

[19] H. Woflson, R. Ahmad, Y. Twig, B. Williams, and A. Blank, "A magnetic resonance probehead for evaluating the level of ionizing radiation absorbed in human teeth," *Health Physics*, vol. 108, no. 3, pp. 326–335, 2015.

[20] C. Bauer, H. Raich, G. Jeschke, and P. Blümler, "Design of a permanent magnet with a mechanical sweep suitable for variable-temperature continuous-wave and pulsed EPR spectroscopy," *Journal of Magnetic Resonance*, vol. 198, no. 2, pp. 222–227, 2009.

[21] G. A. Rinard, R. W. Quine, G. R. Eaton et al., "Magnet and gradient coil system for low-field EPR imaging," *Concepts in Magnetic Resonance*, vol. 15, no. 1, pp. 51–58, 2002.

[22] H. Sato-Akaba, H. Fujii, and H. Hirata, "Development and testing of a CW-EPR apparatus for imaging of short-lifetime nitroxyl radicals in mouse head," *Journal of Magnetic Resonance*, vol. 193, no. 2, pp. 191–198, 2008.

[23] C. P. Poole, *Electron Spin Resonance: A Comprehensive Treatise on Experimental Techniques*, Courier Corporation, Chelmsford, MA, USA, 1996.

[24] P. Fattibene and F. Callens, "EPR dosimetry with tooth enamel: a review," *Applied Radiation and Isotopes*, vol. 68, no. 11, pp. 2033–2116, 2010.

[25] I. Salikhov, T. Walczak, P. Lesniewski et al., "EPR spectrometer for clinical applications," *Magnetic Resonance in Medicine*, vol. 54, no. 5, pp. 1317–1320, 2005.

[26] W. Lee, J. Park, J. Jeong et al., "Analysis of the facial anthropometric data of Korean pilots for oxygen mask design," in *Proceedings of the Human Factors and Ergonomics Society Annual Meeting*, pp. 1927–1931, SAGE Publications, Los Angeles, CA, USA, 2012.

[27] D. Cai, L.-L. Huang, T. Liu, and M. You, "Determining cockpit dimensions and associative dimensions between components in cockpit of ultralight plane for Taiwanese," in *Proceedings of the International Conference on Digital Human Modeling*, pp. 365–374, Springer, Berlin, Germany, 2009.

[28] W. Lee, B. Lee, X. Yang et al., "A 3D anthropometric sizing analysis system based on North American CAESAR 3D scan data for design of head wearable products," *Computers and Industrial Engineering*, vol. 117, pp. 121–130, 2018.

[29] E. J. Dickinson, H. Ekström, and E. Fontes, "COMSOL Multiphysics®: finite element software for electrochemical analysis. A mini-review," *Electrochemistry Communications*, vol. 40, pp. 71–74, 2014.

[30] R. C. B. Brandão and L. B. C. Brandão, "Finishing procedures in orthodontics: dental dimensions and proportions (microesthetics)," *Dental Press Journal of Orthodontics*, vol. 18, no. 5, pp. 147–174, 2013.

[31] J. I. Park, K. Choi, C. U. Koo et al., "Dependence of radiation-induced signals on geometry of tooth enamel using a 1.15 GHz electron paramagnetic resonance spectrometer: improvement of dosimetric accuracy," *Health Physics*, vol. 120, no. 2, pp. 152–162, 2021.

[32] B. D. Cullity and C. D. Graham, *Introduction to Magnetic Materials*, Wiley, Hoboken, NJ, USA, 2011.